



Lautenschlager, S., Figueirido, B., Cashmore, D., Bendel, E-M., & Stubbs, T. L. (2020). Morphological convergence obscures functional diversity in sabre-toothed carnivores. *Proceedings of the Royal Society of London B: Biological Sciences*, 287(1935).  
<https://doi.org/10.1098/rspb.2020.1818>

Peer reviewed version

Link to published version (if available):  
[10.1098/rspb.2020.1818](https://doi.org/10.1098/rspb.2020.1818)

[Link to publication record in Explore Bristol Research](#)  
PDF-document

This is the author accepted manuscript (AAM). The final published version (version of record) is available online via The Royal Society at <https://doi.org/10.1098/rspb.2020.1818>. Please refer to any applicable terms of use of the publisher.

## University of Bristol - Explore Bristol Research

### General rights

This document is made available in accordance with publisher policies. Please cite only the published version using the reference above. Full terms of use are available:  
<http://www.bristol.ac.uk/red/research-policy/pure/user-guides/ebr-terms/>

# PROCEEDINGS OF THE ROYAL SOCIETY B

BIOLOGICAL SCIENCES

## Morphological convergence obscures functional diversity in sabre-toothed carnivores

|                               |   |
|-------------------------------|---|
| Journal:                      | <i>Proceedings B</i>  |
| Manuscript ID                 | RSPB-2020-1818.R1   |
| Article Type:                 | Research  |
| Date Submitted by the Author: | 03-Sep-2020   |
| Complete List of Authors:     | Lautenschlager, Stephan; University of Birmingham, Figueirido, Borja; Universidad de Málaga<br>Cashmore, Daniel; University of Birmingham<br>Bendel, Eva-Maria; Museum für Naturkunde - Leibniz-Institut für Evolutions- und Biodiversitätsforschung; Humboldt-Universität zu Berlin<br>Stubbs, Thomas; University of Bristol, School of Earth Sciences |
| Subject:                      | Palaeontology < BIOLOGY, Evolution < BIOLOGY  |
| Keywords:                     | Convergent evolution, functional morphology, computational analysis, Smilodon, ecology  |
| Proceedings B category:       | Palaeobiology   |
|                               |   |

SCHOLARONE™  
Manuscripts

**Author-supplied statements**

Relevant information will appear here if provided.

***Ethics***

*Does your article include research that required ethical approval or permits?:*

This article does not present research with ethical considerations

*Statement (if applicable):*

CUST\_IF\_YES\_ETHICS :No data available.

***Data***

*It is a condition of publication that data, code and materials supporting your paper are made publicly available. Does your paper present new data?:*

Yes

*Statement (if applicable):*

All data files are available via the following link:

<https://beardatashare.bham.ac.uk/getlink/fiR7wvK357hbPrQ9FVg6eR1Q/> Upon acceptance the files will be moved to a permanent repository (e.g. Dryad, Zenodo; depending on journal integration policy).

***Conflict of interest***

I/We declare we have no competing interests

*Statement (if applicable):*

CUST\_STATE\_CONFLICT :No data available.

***Authors' contributions***

This paper has multiple authors and our individual contributions were as below

*Statement (if applicable):*

S.L conceived the study and designed the analyses. S.L., D.D.C and T.L.S. conducted the analyses and designed the figures. B.F and E.-M.B. contributed to the datasets. All authors contributed to the writing of the manuscript

1 **Morphological convergence obscures functional diversity in sabre-toothed**  
2 **carnivores**

3  
4 Stephan Lautenschlager<sup>1</sup>, Borja Figueirido<sup>2</sup>, Daniel D. Cashmore<sup>1</sup>, Eva-Maria Bendel<sup>3,4</sup>, Thomas L.  
5 Stubbs<sup>5</sup>

6  
7 <sup>1</sup>School of Geography, Earth and Environmental Sciences, University of Birmingham, Edgbaston,  
8 Birmingham B15 2TT, UK

9 <sup>2</sup>Universidad de Málaga, Departamento de Ecología y Geología, Facultad de Ciencias, 29071-  
10 Málaga, Spain.

11 <sup>3</sup>Museum für Naturkunde, Leibniz-Institut für Evolutions- und Biodiversitätsforschung,  
12 Invalidenstraße 43 10115 Berlin, Germany

13 <sup>4</sup>Institut für Biologie, Humboldt-Universität zu Berlin, Invalidenstraße 42, 10115 Berlin, Germany

14 <sup>5</sup>School of Earth Sciences, University of Bristol, 24 Tyndall Avenue, Bristol BS8 1TQ, U.K.  
15

16 **The acquisition of elongated, sabre-like canines in multiple vertebrate clades during the last**  
17 **265 million years represents a remarkable example for convergent evolution. Due to striking**  
18 **superficial similarities in the cranial skeleton, the same or similar skull and jaw functions**  
19 **have been inferred for sabre-toothed species and interpreted as an adaptation to subdue**  
20 **large-bodied prey. However, although some sabre-tooth lineages have been classified into**  
21 **different ecomorphs (dirk-teeth and scimitar-teeth) the functional diversity within and**  
22 **between groups and the evolutionary paths leading to these specialisations are unknown.**  
23 **Here, we use a suite of biomechanical simulations to analyse key functional parameters**  
24 **(mandibular gape angle, bending strength, bite force) to compare the functional performance**  
25 **of different groups and to quantify evolutionary rates across sabre-tooth vertebrates. Our**  
26 **results demonstrate a remarkably high functional diversity between sabre-tooth lineages and**  
27 **that cranial function and prey killing strategies evolved within clades. Moreover, different**  
28 **biomechanical adaptations in coexisting sabre-tooth species further suggest that this**  
29 **functional diversity was at least partially driven by niche-partitioning.**

30 **Key words:** Convergent evolution, functional morphology, computational analysis, *Smilodon*,  
31 ecology  
32

## 33 **1. Introduction**

34 The sabre-toothed cat *Smilodon fatalis* from the Pleistocene of North America represents one of the  
35 most iconic and instantly recognisable vertebrate fossils [1]. Its distinct morphology characterised by  
36 the eponymous, elongated canine teeth, has received considerable academic and public attention [2-  
37 4]. However, sabre-toothed species were much more diverse and widespread in the fossil record than  
38 the prominence of this single well-known species would suggest. Although only loosely defined and  
39 not equally distributed across different species, sabre-tooth morphologies, such as elongate and  
40 mediolaterally flattened canines, an often anteroposteriorly compressed braincase, and a reduced  
41 coronoid process, have evolved several times convergently: in metatherians (thylacosmilines), in  
42 eutherians (independently in creodonts, nimravids, barbourfelids, and machairodontine felids), and  
43 outside of Mammalia in Permian gorgonopsians [5,6] (figure 1).

44 Through time, sabre-toothed carnivores showed a near-global distribution across North  
45 America, Europe, Africa and Asia and dominated many terrestrial ecosystems during the Permian  
46 and the Cenozoic [1,7]. This repeated occurrence of sabre-toothed morphologies in different, and  
47 often unrelated, groups separated by up to 200 million years has been explained with independent  
48 adaptations for subduing large-bodied prey [5,8 although see 9]. Furthermore, the presence of sabre-  
49 toothed characters has been hypothesised to provide distinct functional advantages [10], which are  
50 thought to represent functional optimisation and trend towards increasingly specialized  
51 feeding/hunting adaptations in each lineage [11].

52 Several characters have been discussed as performance indicators in sabre-toothed taxa,  
53 including the evolution of a large jaw gape, decreased or increased bite forces and improved stability  
54 of the craniodental complex [4,12-14]. However, functional studies of sabre-toothed predators have  
55 often focused on single well-known or well-preserved species within each lineage, and these have  
56 usually been the most derived taxa impeding inferences about evolutionary trajectories [4,5,13]. This  
57 traditional focus on derived taxa has further led to the assumption of functional and evolutionary  
58 convergence across sabre-toothed forms. However, caution is warranted over simplified

59 morphological comparisons, as morphological convergence can be a poor indicator for functional  
60 convergence [15,16]. Nevertheless, similar ecomorphologies, prey selection, hunting and killing  
61 behaviour have been suggested for all sabre-tooths, although some functional differences between  
62 scimitar-toothed and dirk-toothed taxa have been recognised [5,6,14,17,18].

63 Here, we investigate the evolution of sabre-toothed morphologies across different clades and  
64 over the last 265 million years from a biomechanical perspective. We test the hypothesis that  
65 functional trends were decoupled and divergent from morphologically convergent trajectories.  
66 Specifically, we obtain biomechanical performance measures (jaw gape, mandibular stability, bite  
67 force), which have been demonstrated to correlate with known biologically and ecologically  
68 meaningful properties [19-21]. Using a combination of biomechanical modelling and phylogenetic  
69 comparative methods, we find that most of the sabre-tooth clades evolved towards different functional  
70 specialisations acquired via variable evolutionary pathways.

71

## 72 **2. Material and methods**

### 73 **(a) Specimen selection**

74 A total of 66 species were sampled from the literature and analysed (see supplementary material)  
75 (figures 1, S1a). Only taxa which preserved the complete craniomandibular skeleton were selected,  
76 as well as a few incomplete taxa, which could be reconstructed with minimal interpretation. This  
77 allowed for over 50% of established species and over 70% of established genera to be sampled in  
78 each group. Two-dimensional outlines of each specimen were generated using Adobe Illustrator CC  
79 (Adobe Inc.) (figure S1b) and muscle attachment sites of the masseter and the temporalis muscle  
80 groups were mapped onto the cranial outlines (the pterygoideus group was not considered due to its  
81 largely mediolateral line of action and negligible contribution to gape angle and bite force) for the  
82 mammalian taxa. For the gorgonopsian taxa, the m. adductor mandibulae externus (m. AME)  
83 complex, the pterygoideus muscles and the pseudotemporalis muscles were each considered as a  
84 single functional unit.

85

86 **(b) Gape analysis**

87 For the gape analysis, the images of the cranial outlines were imported into Blender

88 ([www.blender.org](http://www.blender.org), version 2.79) to generate simplified skull and jaw models (figure S1c) using a

89 box-modelling approach [22]. The outlines were extruded in the third dimension by a consistent

90 width of 2 mm (we refer to these simplified three-dimensional models as extruded models following

91 [23]).

92 The gape analysis (figures 2, S1d) followed the methodology detailed in [24]. The skull and

93 mandible models were joined at the jaw joint and the mandible was allowed full rotation around the

94 mediolateral axis (y-axis) to simulate sagittal opening and closing. Adductor muscles were

95 represented by cylinders connecting the attachment sites projected onto the extruded models. An

96 opening motion with a step size of 0.5 degrees was imposed on the lower jaw, during which the

97 muscle cylinders were stretched. For each step, the ratio between the resting length and the

98 extended length of the muscle cylinders was calculated until any of the muscle cylinders reached

99 the critical extension limit of 170%. This extension limit was based on experimentally derived

100 values for mammalian adductor muscles above which tetanic tension of muscles is no longer

101 possible [24]. Although it cannot be ruled out that the non-mammalian taxa in this study had a

102 different muscle architecture, the same extension limit was assumed for consistency.

103 To test whether the extruded models could faithfully reproduce realistic results, the

104 methodology was validated using three-dimensional models of fossil sabre-tooths (*Smilodon fatalis*,105 *Homotherium serum*, *Yoshi garevskii*, *Inostrancevia alexandri*) and extant felids (*Panthera leo*,106 *Hyena hyena*), which covered the range of observed cranial morphologies (see supplementary

107 material). To further account for uncertainties regarding the exact muscle attachment, five different

108 variations in muscle arrangement were tested for each model and the average gape angle was

109 calculated. To evaluate how much the extruded models underestimate gape angles, a correction

110 factor was calculated (see supplementary material, figures S2-4). The obtained correction factor of  
111 2.0 was then applied to the results from the extruded models.

112

### 113 **(c) Finite element analysis**

114 To assess the biomechanical performance of the studied taxa, finite element analyses (FEA) were  
115 performed (S1e). In comparison with full 3D models, the extruded models may not capture the full  
116 biological signal. However, it has been demonstrated that meaningful, shape-related biomechanical  
117 performance measures can be obtained from extruded models [23,25-28]. Sensitivity tests were  
118 performed by comparing FEA results obtained from corresponding extruded and full 3D models for  
119 selected taxa (see supplementary material, figures S5, S6). Only the mandible morphology was  
120 considered for FEA, as it can be more accurately replicated in this simplified context. Furthermore,  
121 the mandible provides a more reliable signal for feeding performance compared to the skull, which  
122 underlies constraints due to compromising functions [21].

123 For FEA, the extruded models of the lower jaws were exported from Blender as .STL files  
124 and imported into HyperMesh (Altair, version 11) for solid meshing and the setting of boundary  
125 conditions. Mesh size was kept uniform to generate a quasi-ideal mesh following [29] (table S1),  
126 which allowed the calculation of average stress values. All models were assigned isotropic material  
127 properties for bone ( $E = 13.7$  GPa,  $\nu = 0.3$ ) and teeth ( $E = 38.6$  GPa,  $\nu = 0.4$ ) [18]. Only the crowns  
128 of the canine teeth were considered in each model, representing the functional unit during initial  
129 prey contact.

130 Two functional scenarios were tested: (i) A non-masticatory bending test to investigate  
131 mandibular stability under generalized loading conditions [21]. A single ventrally directed nodal  
132 force was applied to the tip of the canine tooth. Load forces were scaled following the quasi-  
133 homothetic transformation approach of [30] which ensures correct force/surface area scaling for  
134 extruded models as used here. Models were further constrained from movement in x-, y- and z-  
135 direction at the jaw joint (three nodes). (ii) A second set of analyses were performed with all



136 mandibles scaled to the same size and adductor muscle forces applied. Adductor muscle forces were  
137 calculated from the size of the attachment area visible in lateral view multiplied by the specific  
138 tension ( $0.3\text{N}/\text{mm}^2$ ) [31]. All models were further constrained from movement at the tip of the  
139 canine tooth (one node in x- and y-direction, but not z-direction to simulate penetration of the prey  
140 by the canine).

141 All models were imported into Abaqus (Simulia, version 6.141) for analysis and post-  
142 processing. Biomechanical performance was assessed by per element average von Mises stress  
143 (with top 1% of magnitudes values excluded to account for artefacts resulting from point loads) and  
144 reaction forces measured at the tip of the canine tooth. Tests for statistical significance of the  
145 individual performance metrics were performed in PAST 3.22 [32] (tables S2-4).

146

#### 147 **(d) Geometric morphometric analysis**

148 To quantify the morphological variation of the analysed taxa, a two-dimensional, landmark-based  
149 geometric morphometrics (GMM) approach was used (figure S1f). A set of fixed landmarks and  
150 semi-landmarks were used to describe the morphology of the skull (8 fixed, 55 semi-landmarks)  
151 and the mandible (6 fixed, 25 semi-landmarks) (figure S7), digitised with tpsDig2 [33]. Landmark  
152 coordinates were subsequently superimposed using a Procrustes Analysis and then subjected to a  
153 Principal Component Analysis (PCA) in PAST 3.22 [32]. PCA scores were used to create  
154 morphospace plots (figures S8-10) and to generate performance heatmaps (figure S1i) using the R  
155 package MBA (<https://cran.r-project.org/web/packages/MBA/index.html>). Phylomorphospaces  
156 were created using the phylogenetic relationships depicted in figure 1.

157

#### 158 **(e) Phylogeny and evolutionary rates**

159 Time-scaled phylogenetic trees with branch lengths were required to investigate the tempo and  
160 mode of biomechanical evolution (figure S1h). Tree topologies are composite phylogenies, based  
161 on [34,35] for sabre-toothed mammals and [36] for gorgonopsians. The individual sabre-toothed

162 mammal topologies were combined into a single composite tree for the rates analyses. We use the  
163 ‘equal’ [37] and the fossilized birth–death (FBD) [38,39] time-scaling approaches to test for  
164 consistency. Temporal data were based on first appearance dates (FADs) and last appearance dates  
165 (LADs), representing the bounds of geological intervals that taxa occurred within. Dating  
166 uncertainty was incorporated when time-scaling trees by running 100 iterations and, for each  
167 iteration, drawing a single occurrence date for each taxon from a uniform distribution between their  
168 FAD and LAD. Traitgrams (phenograms) (figure S11) were generated for each biomechanical  
169 character for each subgroup using a randomly selected time-calibrated tree for each group, and  
170 maximum-likelihood ancestral state estimation in phytools [40].

171 Rates of biomechanical evolution were analysed using a Bayesian approach with the  
172 variable-rates model in BayesTraits v. 2.0.2 [41]. For the 100 time-scaled iterations of the  
173 gorgonopsian tree and the full sabre-toothed mammal tree, rate heterogeneity in each  $\log_{10}$   
174 transformed character was tested using a reversible jump Markov Chain Monte Carlo algorithm  
175 (rjMCMC). Each tree was run for 200 million iterations, parameters were sampled every 16,000  
176 iterations and the first 40 million iterations were discarded as burn-in. The smallest effective sample  
177 size (ESS) was used to assess run convergence. To detect shifts in evolutionary rates, the variable-  
178 rates model rescales branches where variance of trait evolution differs from that expected in a  
179 homogeneous (Brownian motion) model. The resulting ‘rate scalars’ represent the amount of  
180 evolutionary acceleration or deceleration relative to the background rate along each branch [41,42].  
181 Stepping-stone sampling, with 100 stones each run for 1000 iterations, was used to calculate the  
182 marginal likelihood of the models (heterogeneous versus homogeneous rates) [43]. Model fit was  
183 compared using Bayes Factors and the Variable Rates Post Processor was used to extract the final  
184 parameter values [42]. We summarised rates results for each character by calculating consensus  
185 trees from all time-scaled trees that favoured a heterogeneous rates model - giving the mean rate  
186 scalars for each branch across gorgonopsians and sabre-toothed mammal phylogeny. Results were  
187 consistent in both the ‘equal’ (figure 4) and FBD dated trees (figure S12).

188

189 **3. Results**190 **(a) Maximum jaw gape**

191 The biomechanical analyses demonstrate that gape angles vary considerably between species and  
192 groups (figure 2a, S9b). Although there appears to be a trend for the increase (barbourofelids,  
193 smilodontines, homotherines) or decrease (nimravids, metailurines) of gape angles through time  
194 none of these relationships are statistically significant (table S2). All species across the different  
195 lineages show gape angles between 52 and 111 degrees, but diversification patterns differ  
196 considerably between groups. Gorgonopsians and nimravids show an “early high disparity” pattern  
197 and the widest range of gape values, indicating an early and fast diversification. All other groups  
198 exhibit a constant to “late high disparity” trend (figure S12a). Effective gape angles (= clearance  
199 between upper and lower canines and a proxy for prey size [9]), are considerably lower than the  
200 maximum gape angles in all groups (figure 2a) but again no statistically significant relationship  
201 through time was recovered (table S2). A comparison between actual and effective gape shows a  
202 (statistically significant) moderate correlation in homotherines ( $R^2 = 0.78$ ,  $p = 6.22E^{-5}$ ) and  
203 nimravids ( $R^2 = 0.65$ ,  $p = 0.0009$ ) but a more decoupled relationship in the other groups ( $R^2 = 0.38$ -  
204 0.63) (table S2, figure S13a).

205 The performance heatmap for the gape angle shows an equal complexity in the evolutionary  
206 dynamics. Some (but not all) derived taxa in each group occupy regions of higher performance  
207 compared to basal forms (for example in gorgonopsians, barbourofelids, and smilodontines).  
208 However, this is not a uniform trend and exceptions are present in each group (figure 3b, S14b, 15b)  
209 with derived taxa moving towards low-performance regions. For effective gape angles (figure 3c),  
210 there is movement between areas of similar performance or towards areas of lower performance  
211 than for the basal taxa in each group (figures 3c, S14c, 15c)

212 Evolutionary rates in jaw gape are heterogeneous for gorgonopsians in the majority of trees  
213 analysed (97%). Rapid rates are concentrated in derived rubidgeines, particularly the robustly

214 skulled and large-bodied *Leontosaurus*, *Dinogorgon*, *Rubidgea* and *Clelandina* (figure 4a).  
215 *Clelandina* evolved the largest gape angle of all gorgonopsians, whilst *Dinogorgon* and  
216 *Leontosaurus* rank amongst the smallest gapes. Similarly, divergent gape angles in closely related  
217 taxa are seen in the *Inostrancevia* (large gape) + *Sauroctonus* (small gape) clade – which also  
218 exhibit moderately fast rates. In mammalian sabre-toothed taxa, there is mixed evidence for  
219 heterogeneous rates, with only 58% of analytical iterations recovering positive evidence for rate  
220 variation (figure 4b). In these trees, rapid rates are seen in smilodontines (*Megantereon*, *Smilodon*),  
221 derived barbourfelids and nimravids (*Pogonodon*, *Hoplophoneus*, *Eusmilus*).

222

### 223 (b) Bending strength

224 Bending strength of the mandible was found to significantly increase with time in barbourfelids  
225 and metailurines (figure 2b, S16). While nimravids and homotherines also show an increase in  
226 bending strength, this trend is not supported statistically. Similarly, the apparent decrease in  
227 gorgonopsians and smilodontines is not statistically significant (figure 2b, table S2). Bending  
228 strength follows a distinct “early high disparity” pattern in nimravids and (to a lesser degree) in  
229 gorgonopsians and also smilodontines. All other groups show a “late high disparity” trend (Fig.  
230 S9b). Overall, bending strength is not correlated with actual gape ( $R^2 < 0.2$ ) and effective gape ( $R^2$   
231  $< 0.47$ ) (table S3, figure S13b, d).

232 Similar to gape angle, the evolutionary trends across the performance heatmap show  
233 complex movement towards different performance areas (figure 3d, S14d, S15d). As recovered  
234 above, only in barbourfelids and metailurines there is a clear trend of derived taxa moving towards  
235 high-performance areas.

236 Rates of evolution in bending strength are generally homogeneous for gorgonopsians, with  
237 only 20% of iterations showing heterogeneity. In contrast, mammalian sabre-toothed taxa show  
238 several bursts of fast evolution in bending strength in 97% of trees. Fast rates are seen in  
239 smilodontines and on internal branches uniting metailurines and smilodontines (figure 4c). This

240 reflects both great disparity in smilodontines (e.g. *Smilodon populator* versus *Smilodon fatalis*) and  
241 the larger difference between generally high bending resistances in smilodontines compared to low  
242 bending strengths in basal metailurines (figure S11b). Elsewhere, rapid rates are seen in sister taxa  
243 that have divergent bending strengths, notably *Homotherium serum* and *Homotherium*  
244 *venezuelensis*, and the nimravids *Eusmilus* and *Hoplophoneus cerebralis* (figure 4c).

245

### 246 (c) Bite force

247 Barbourfelids and metailurines show a statistically significant trend of decreasing bite forces  
248 through time Other groups appear to have a constant (nimravids, homotherines) or increased  
249 (gorgonopsians, smilodontines) bite force through time, but these trends are not statistically  
250 supported (figures 2c, S17, table S2). Gorgonopsians explore a wider range of relative bite forces  
251 (ca. 15-35%), while the mammalian sabre-tooths are restricted to lower relative bite forces (ca. 10-  
252 25%). No or only weak and statistically not significant correlations were found between bite force  
253 and actual gape ( $R^2 < 0.04$ ) and bite force and effective gape ( $R^2 < 0.3$ ), whereas a moderate  
254 correlation between bending strength and bite force is observed in barbourfelids ( $R^2 = 0.77$ ,  $p =$   
255  $0.03$ ) and metailurines ( $R^2 = 0.54$ ,  $p = 0.026$ ) (table S3, figure S13c, e, f).

256 The evolutionary pathways across the performance space show that selected derived taxa in  
257 some groups (gorgonopsians, smilodontines) move towards areas of higher performance compared  
258 to the basal taxa. However, this trend is not consistent for all derived taxa in these groups. In  
259 contrast, barbourfelids and metailurines move towards low-performance areas (figures 3e, S14e,  
260 S15e).

261 In gorgonopsians, again only 11% of iterations show evidence for rate variation, suggesting  
262 that a homogeneous rate (Brownian motion) model is favoured. Accelerated rates of bite force  
263 evolution were widely distributed in mammalian sabre-toothed taxa (figure 4d) and a heterogeneous  
264 rates model is favoured for 94% of analysed trees. Fastest rates are seen in nimravids, particularly  
265 *Eusmilus* and *Hoplophoneus*. Other high rate instances involve taxa that evolved contrasting bite

266 forces compared to their closest relatives. This is seen in homotherines, where *Amphimachairodus*  
267 evolved relatively large bite forces, in metailurines, where *Dinofelis* shows notably smaller bite  
268 forces than more basal taxa, and in smilodontines, where *Megantereon* has increased bite force  
269 relative to others.

270

#### 271 4. Discussion

272 The acquisition of hypertrophied canine teeth and cranial sabre-tooth characteristics across different  
273 vertebrate lineages represents a remarkable example of convergent evolution [11]. Despite the close  
274 morphological similarities exhibited by individual groups/species, some more general  
275 differentiations have been discussed for derived sabre-tooth felids [44,45]: scimitar-toothed cats  
276 (i.e. homotherines) with relatively shorter, broad and coarsely-serrated canines and dirk-toothed cats  
277 (i.e. smilodontines) with elongate and finely or unserrated canines, each representing a distinct  
278 ecomorphology with different cranial functions, as well as differences in their postcranial anatomy  
279 [46]. Our new analyses demonstrate that morphofunctional differences and evolutionary dynamics  
280 of synapsid sabre-teeth are far more complex. Rather than a clear dichotomous split into two  
281 ecomorphologies, we observe a spectrum of functional adaptations. **Derived from the combination**  
282 **of the analysed functional parameters (actual and effective gape angle, bending strength, bite force),**  
283 **there are no two clades showing the same distribution of parameters and evolutionary rates (figures**  
284 **2-4, S14, S15).** This confirms assumptions from previous studies on tooth morphology, bite-depth  
285 and postcranial specialisations that sabre-tooth function and prey killing strategies evolved along  
286 functionally diverse pathways [9,14,18,47]. Discoveries of mosaic-taxa, such as *Xenosmilus*  
287 *hodsonae*, combining scimitar- and dirk-toothed characteristics, had already hinted at the existence  
288 of wider morphofunctional diversity [48]. However, it should be noted that only about a fraction of  
289 the functional trends through time have been recovered as statistically significant (table S2).  
290 **This is likely an effect of the divergent functional performances of derived taxa in each group**  
291 **(figure S11) as well as due to the lack of stratigraphic resolution resulting in the same/similar first**

292 appearance dates (in particular for gorgonopsians). In all groups, an increase of functional diversity  
293 due to the exploration of different functionspace regions (figure S11) can be observed in the derived  
294 taxa which likely dilutes overall trends but lends further proof to the wide diversity of functional  
295 adaptations. Consequently, we find no proof for linear functional optimisation of groups as a whole.

296 Generally, the analyses reveal the emergence of individual species and morphologies with  
297 high performances through time but with broad functional diversity and widely distributed high  
298 rates leading to functional divergence in each group. For example, an adoption of increased jaw  
299 gape and mandibular bending strength is found in most groups, as would be expected following the  
300 cranial modifications (i.e. rotation of the braincase, reduction of coronoid process, mental process).

301 While actual gape angles show a range of ca. 60 degrees (reaching up to 111 degrees in *Smilodon*  
302 *fatalis*), effective gape is restricted to a maximum of ca. 70 degrees, with most species ranging  
303 between 45 and 65 degrees. This is a similar clearance observed in modern felids [5] and appears to  
304 be the most effective gape necessary for prey capture casting further doubt on the idea of all sabre-  
305 teeth being large prey specialists [9]. The significant correlation between actual and effective gape  
306 in nearly all groups (table S3) suggests that canine length and jaw gape are equally important  
307 factors and that canine penetration is more important than maximising prey size [9].

308 Interestingly, within gorgonopsians, the majority of taxa shows actual gape angles below 80  
309 degrees and effective gape angles below 60 degrees suggesting a possible specialisation towards  
310 smaller rather than larger prey, possibly as a strategy to conserve energy expenditure [49]. It is,  
311 therefore, possible that the sabre-like canines in gorgonopsians were used to inflict more severe  
312 wounds in smaller/similar-sized prey or had an additional function independent of feeding [50,51].  
313 Positioned considerably outside of mammalian synapsids, gorgonopsians were not constrained in  
314 their cranial function by a generalised mammalian/carnivoran morphology. In fact, re-modelling of  
315 the skull and jaw (e.g. rotation of the facial skeleton, compaction of the braincase, reduction in jaw  
316 adductor space, reduction of the coronoid process, increased attachment for post-cranial  
317 musculature) is largely absent in gorgonopsians [5]. Furthermore, the gorgonopsian bite technique

318 is significantly dissimilar to that of eutherians: Gorgonopsians used a kinetic-inertial jaw-closing  
319 system (analogue to modern crocodylians) relying predominantly on the pterygoideus and  
320 temporalis muscle groups to deliver powerful and fast jaw closure [6]. However, the taxa included  
321 in our analyses do not account for the entire diversity in gorgonopsian morphology but include  
322 mostly larger taxa (e.g. Russian species as well as the morphologically advanced Rubidgeinae [52]).  
323 Gorgonopsians only show evolutionary bursts in gape evolution within derived rubidgeines, but bite  
324 force and bending strength evolved following a homogeneous rates model. This result may, in part,  
325 be due to a low sample size for this group and failure to detect rate variation.

326 While there appears to be a trend towards increased relative bite forces in gorgonopsians and  
327 smilodontines, only the decrease of relative bite force through time in barbourofelids and  
328 metailurines is statistically supported. This seemingly counterintuitive trend in barbourofelids may  
329 be explained with the increasing specialisation and evolution of a novel prey killing strategy in  
330 derived taxa. With a shift from a killing bite (similar to modern felids) powered by the jaw muscles,  
331 to a canine-shear bite harnessing the neck musculature [45, 47, 53] bite-force becomes less  
332 important. At the same time, the emphasis on large jaw gape and canine clearance requires a  
333 reorganisation of the jaw adductor musculature changing the mechanical advantage and therefore  
334 constraining the ability to produce high bite forces [4,5,13].

335 The canine-shear bite has also been accepted as the main killing mode in *Smilodon fatalis*  
336 and other smilodontines [3,13]. However, while derived smilodontines have among the highest  
337 actual gape angles, bite forces are not decreasing through time as in barbourofelids. This may be  
338 because relative bite forces are within a similar range in derived smilodontines (ca. 15-20 degrees)  
339 to those in derived barbourofelids (ca. 12-17 degrees). A canine-shear bite is therefore likely to be  
340 the main killing style in both groups. However, the lower bending strength of the mandible in  
341 derived smilodontines would have, in contrast to barbourofelids with their prominently developed  
342 mental processes, required more powerful forelimbs to restrain prey [8,10,47]. Metailurines parallel  
343 barbourofelids closely in increasing mandibular bending strength and decreasing relative bite forces



344 through time. However, metailurines do not show the extent of cranial and mandibular  
345 modifications indicative of a canine-shear bite. It is, therefore, possible, that these trends reflect an  
346 adaptation to small prey in derived metailurines. In contrast, homotherines would have engaged in a  
347 different killing technique as indicated by moderate values and no significant changes through time  
348 of all functional parameters. Homotherines likely employed a predatory behaviour between a  
349 clamp-and-hold bite (analogue to modern pantherines) and a canine-shear bite as suggested by  
350 previous morphological and biomechanical analyses [18,48]. Nimravids generally show high jaw  
351 gapes (i.e. majority of taxa with actual gape angles over 90 degrees) and bending strength values  
352 with little change through time. This could represent an intermediate killing strategy for nimravids  
353 (as previously hypothesised based on the analysis of mandibular force profiles) [10] with a  
354 specialisation towards large-bodied prey [47] for which large gape angles and bending strength  
355 would be necessary.

356 The evolutionary pathways across the performance heatmaps (figure 3) further support the  
357 hypothesis that the different sabre-tooth species and groups pursued different hunting/killing  
358 strategies. However, they also show that there is no single consistent trend towards functional  
359 optimisation as hypothesised in the past [11]. All analysed groups span a wide range between basal  
360 and derived members across the heatmaps/morphospace. With the exception of metailurines, which  
361 are restricted to small areas of the mandibular, cranial and combined morphospaces, all groups can  
362 be found expanding into different regions of the morphospace (figures 3a, S14a, S15a).

363 Anatomically, this represents an adoption of “typical sabre-tooth” morphologies (i.e.  
364 anteroposteriorly short but dorsoventrally high skulls, a reduced coronoid process, an expanded  
365 mental process) towards one end and the retention of “cat-like” morphologies (i.e. relatively shorter  
366 canines, low braincase, high coronoid process) on the other end (figures 3a, S14a, S15a). Again,  
367 gorgonopsians form the exception in occupying mostly distinct areas in the morphospace, with only  
368 occasional intrusions into the areas occupied by the mammalian taxa (figures 3a, S15a). This

369 pattern further supports the assumption that felid sabre-teeth were highly specialised but  
370 morphofunctionally constrained, possibly due to a high degree of functional integration [35].

371 It is further noteworthy that metailurines, homotherines and smilodontines show different or  
372 even opposing functional performances and that divergent functional morphologies are linked to  
373 rapid evolutionary shifts in some derived taxa in each group (figure 4). These three groups had  
374 considerable spatial and temporal overlap with several sabre-tooth species sharing the same  
375 ecosystem with each other and other mammalian carnivores [54,55]. Fast rates and different  
376 functional performances, therefore, suggest selective pressures, considerable specialisation and  
377 niche-partitioning to avoid intra- and interclade competition. Our results parallel previous findings  
378 that mandible shape in sabre-toothed cats evolved at a higher rate than in modern conical toothed  
379 cats [34]. This demonstrates that although a large degree of morphological convergence is present  
380 in these groups, functional characteristics are much more variable and diverse.

381 **References**

- 382 1. Werdelin, L., McDonald, H. G., & Shaw, C. A. *Smilodon: The Iconic Sabretooth*. (JHU  
383 Press, 2018).
- 384 2. Warren, J. C. Remarks on *Felis Smylodon*. *Proceedings of the Boston Society of Natural*  
385 *History*. IV, 256–258 (1853).
- 386 3. Akersten, W.A. Canine function in *Smilodon* (Mammalia; Felidae; Machairodontinae).  
387 *Contributions to Science of the Natural History Museum Los Angeles*. **356**, 1–22 (1985).
- 388 4. McHenry, C.R., Wroe, S., Clausen, P.D., Moreno, K. & Cunningham, E. Supermodeled  
389 sabrecat, predatory behavior in *Smilodon fatalis* revealed by high-resolution 3D computer  
390 simulation. *Proceedings of the National Academy for Science*. **104**, 16010–16015 (2007).
- 391 5. Emerson, S. B. & Radinsky, L. B. Functional analysis of sabretooth cranial morphology.  
392 *Paleobiology*. **6**, 295–312 (1980).
- 393 6. Van Valkenburgh, B. & Jenkins, I. Evolutionary patterns in the history of Permo-Triassic  
394 and Cenozoic synapsid predators. *Paleontological Society Papers*. **8**, 267–288 (2002).
- 395 7. Christiansen, P. Phylogeny of the sabretoothed felids (Carnivora: Felidae:  
396 Machairodontinae). *Cladistics*, **29**, 543-559 (2013).
- 397 8. Meachen-Samuels, J. A. & Van Valkenburgh, B. Radiographs reveal exceptional forelimb  
398 strength in the sabretooth cat, *Smilodon fatalis*. *PLoS One*, **5**, e11412 (2010).
- 399 9. Andersson, K., Norman, D. & Werdelin, L. Sabretoothed carnivores and the killing of  
400 large prey. *PLoS One*, **6**, e24971 (2011).
- 401 10. Therrien, F. Feeding behaviour and bite force of sabretoothed predators. *Zoological Journal*  
402 *of the Linnean Society*, **145**, 393-426 (2005).
- 403 11. Van Valkenburgh, B. Déjà vu: the evolution of feeding morphologies in the Carnivora.  
404 *Integrative and Comparative Biology*, **47**, 147-163 (2007).
- 405 12. Antón, M., & Galobart, À. Neck function and predatory behavior in the scimitar toothed cat  
406 *Homotherium latidens* (Owen). *Journal of Vertebrate Paleontology*, **19**, 771-784 (1999).

- 407 13. Christiansen, P. Comparative bite forces and canine bending strength in feline and  
408 sabretooth felids: implications for predatory ecology. *Zoological Journal of the Linnean*  
409 *Society*, **151**, 423-437 (2007).
- 410 14. Slater, G. J., & Van Valkenburgh, B. Long in the tooth: evolution of sabretooth cat cranial  
411 shape. *Paleobiology*, **34**, 403-419 (2008).
- 412 15. Losos, J. B. Convergence, adaptation, and constraint. *Evolution*, **65**, 1827-1840 (2011)
- 413 16. Lautenschlager, S., Brassey, C. A., Button, D. J., & Barrett, P. M. Decoupled form and  
414 function in disparate herbivorous dinosaur clades. *Scientific Reports*, **6**, 26495 (2016).
- 415 17. Figueirido, B., MacLeod, N., Krieger, J., De Renzi, M., Pérez-Claros, J. A., & Palmqvist, P.  
416 Constraint and adaptation in the evolution of carnivoran skull shape. *Paleobiology*, **37**, 490-  
417 518 (2011).
- 418 18. Figueirido, B., Lautenschlager, S., Pérez-Ramos, A., & Van Valkenburgh, B. Distinct  
419 Predatory Behaviors in Scimitar-and Dirk-Toothed Sabretooth Cats. *Current Biology*, **28**,  
420 3260-3266 (2018).
- 421 19. Pierce, S. E., Angielczyk, K. D., & Rayfield, E. J. Patterns of morphospace occupation and  
422 mechanical performance in extant crocodylian skulls: a combined geometric morphometric  
423 and finite element modeling approach. *Journal of Morphology*, **269**, 840-864 (2008).
- 424 20. Polly, P. D., Stayton, C. T., Dumont, E. R., Pierce, S. E., Rayfield, E. J., & Angielczyk, K.  
425 D. Combining geometric morphometrics and finite element analysis with evolutionary  
426 modeling: towards a synthesis. *Journal of Vertebrate Paleontology*, **36**, e1111225 (2016).
- 427 21. Tseng, Z. J., & Flynn, J. J. Structure-function covariation with nonfeeding ecological  
428 variables influences evolution of feeding specialization in Carnivora. *Science Advances*, **4**,  
429 eaao5441 (2018).
- 430 22. Rahman, I. A., & Lautenschlager, S. Applications of three-dimensional box modeling to  
431 paleontological functional analysis. *The Paleontological Society Papers*, **22**, 119-132  
432 (2016).

- 433 23. Morales-García, N. M., Burgess, T. D., Hill, J. J., Gill, P. G. & Rayfield, E. J. The use of  
434 extruded finite-element models as a novel alternative to tomography-based models: a case  
435 study using early mammal jaws. *Journal of the Royal Society Interface*, **16**, 20190674  
436 (2019).
- 437 24. Lautenschlager, S. Estimating cranial musculoskeletal constraints in theropod dinosaurs.  
438 *Royal Society Open Science*, **2**, 150495 (2015).
- 439 25. Fletcher, T. M., Janis, C. M., & Rayfield, E. J. Finite element analysis of ungulate jaws: can  
440 mode of digestive physiology be determined. *Palaeontologia Electronica*, **13**, 1-15 (2010).
- 441 26. Young, M. T., Brusatte, S. L., Ruta, M. & de Andrade, M. B. The evolution of  
442 Metriorhynchoidea (Mesoeucrocodylia, Thalattosuchia): an integrated approach using  
443 geometric morphometrics, analysis of disparity, and biomechanics. *Zoological Journal of*  
444 *the Linnean Society*, **158**, 801-859 (2010).
- 445 27. Neenan, J. M., Ruta, M., Clack, J. A. & Rayfield, E. J. Feeding biomechanics in  
446 *Acanthostega* and across the fish–tetrapod transition. *Proceedings of the Royal Society B:*  
447 *Biological Sciences*, **281**, 20132689 (2014).
- 448 28. Serrano-Fochs, S., De Esteban-Trivigno, S., Marcé-Nogué, J., Fortuny, J., Fariña, R.A..  
449 Finite Element Analysis of the Cingulata Jaw: An Ecomorphological Approach to  
450 Armadillo’s Diets. *PLoS One* **10**, e0120653 (2015).
- 451 29. Marcé Nogué, J., de Esteban-Trivigno, S., Escrig Pérez, C. & Gil Espert, L. Accounting for  
452 differences in element size and homogeneity when comparing Finite Element models:  
453 Armadillos as a case study. *Palaeontologia Electronica*, **19**, 1-22 (2016).
- 454 30. Marcé-Nogué, J., DeMiguel, D., Fortuny, J., de Esteban-Trivigno, S., Gil, L. Quasi-  
455 homothetic transformation for comparing the mechanical performance of planar models in  
456 biological research. *Palaeontologia Electronica*, **16**, 1-15 (2013).

- 457 31. Thomason, J. J., Russell, A. P., & Morgeli, M. Forces of biting, body size, and masticatory  
458 muscle tension in the opossum *Didelphis virginiana*. *Canadian Journal of Zoology*, **68**, 318-  
459 324 (1990).
- 460 32. Hammer, Ø., Harper, D. A. & Ryan, P. D. PAST: paleontological statistics software package  
461 for education and data analysis. *Palaeontologia Electronica*, **4**, 1-9 (2001).
- 462 33. Rohlf, F.J. TpsDig 2. (Department of Ecology and Evolution. State University of New York,  
463 Stony Brook, NY, 2010)
- 464 34. Piras, P., Silvestro, D., Carotenuto, F., Castiglione, S., Kotsakis, A., Maiorino, L.,  
465 Melchionna, M., Mondanaro, A., Sansalone, G., Serio, C. & Vero, V. A. Evolution of the  
466 sabretooth mandible: A deadly ecomorphological specialization.
- 467 35. Piras, P., Maiorino, L., Teresi, L., Meloro, C., Lucci, F., Kotsakis, T., & Raia, P. Bite of the  
468 cats: relationships between functional integration and mechanical performance as revealed  
469 by mandible geometry. *Systematic Biology*, **62**, 878-900 (2013).
- 470 36. Bendel, E. M., Kammerer, C. F., Kardjilov, N., Fernandez, V. & Fröbisch, J. Cranial  
471 anatomy of the gorgonopsian *Cynariops robustus* based on CT-reconstruction. *PloS one*, **13**,  
472 e0207367 (2018).
- 473 37. Brusatte, S. L., Benton, M. J., Ruta, M. & Lloyd, G. T. Superiority, Competition, and  
474 Opportunism in the Evolutionary Radiation of Dinosaurs. *Science*, **321**, 1485-91488 (2008).
- 475 38. Zhang, C., Stadler, T., Klopstein, S., Heath, T. A., & Ronquist, F. Total-evidence dating  
476 under the fossilized birth–death process. *Systematic Biology*, **65**, 228–249 (2015).
- 477 39. Matzke, N. J., & Wright, A. Inferring node dates from tip dates in fossil Canidae: the  
478 importance of tree priors. *Biology Letters*, **12**, 20160328 (2016).
- 479 40. Revell, L. J. Phytools: an R package for phylogenetic comparative biology (and other  
480 things). *Methods in Ecology and Evolution* **3**, 217-223 (2012).
- 481 41. Venditti, C., Meade, A. & Pagel, M. Multiple routes to mammalian diversity. *Nature* **479**,  
482 393-396 (2011).

- 483 42. Baker, J., Meade, A., Pagel, M. & Venditti, C. Positive phenotypic selection inferred from  
484 phylogenies. *Biological Journal of the Linnean Society*, **118**, 95-115 (2016).
- 485 43. Xie, W., Lewis, P. O., Fan, Y., Kuo, L., & Chen, M. H. Improving marginal likelihood  
486 estimation for Bayesian phylogenetic model selection. *Systematic Biology*, **60**, 150-160  
487 (2011).
- 488 44. Kurten, B. *Pleistocene mammals of Europe*. (Routledge Press, 1968).
- 489 45. Martin, L. D. Functional morphology and the evolution of cats. *Transactions of the*  
490 *Nebraska Academy of Sciences*, **8**, 141-154 (1980).
- 491 46. Anyonge, W. Locomotor behaviour in Plio-Pleistocene sabre-tooth cats: a biomechanical  
492 analysis. *Journal of Zoology*, **238**, 395-413 (1996).
- 493 47. Meachen-Samuels, J. A. Morphological convergence of the prey-killing arsenal of  
494 sabretooth predators. *Paleobiology*, **38**, 1-14 (2012).
- 495 48. Martin, L. D., Babiarz, J. P., Naples, V. L. & Hearst, J. Three ways to be a sabre-toothed cat.  
496 *Naturwissenschaften*, **87**, 41-44 (2000).
- 497 49. Carbone, C. Teacher, A., & Rowcliffe, J. M. The costs of carnivory. *PLoS Biology*, **5**, 1-6  
498 (2007).
- 499 50. Benoit, J., Manger, P. R., Fernandez, V. & Rubidge, B. S. Cranial bosses of *Choerosaurus*  
500 *dejageri* (Therapsida, Therocephalia): earliest evidence of cranial display structures in  
501 eutheriodonts. *PloS One*, **11**, e22 (2016).
- 502 51. Kammerer, C. F. Systematics of the Rubidgeinae (Therapsida: Gorgonopsia). *PeerJ*, **4**,  
503 e1608 (2016).
- 504 52. Kammerer, C. F. & Masyutin, V. Gorgonopsian therapsids (*Nochnitsa* gen. nov. and  
505 *Viatkogorgon*) from the Permian Kotelnich locality of Russia. *PeerJ*, **6**, e4954 (2018).
- 506 53. Martin, L. D., Schultz, C. B. & Schultz, M. R. Sabre-toothed cats from the Plio-Pleistocene  
507 of Nebraska. *Transactions of the Nebraska Academy of Sciences*, **16**, 153-163 (1988).

- 508 54. Hunt Jr, R. M. Biogeography of the order Carnivora. *Carnivore behavior, ecology, and*  
509 *evolution*, **2**, 485-541 (1996).
- 510 55. Van Valkenburgh, B. Major patterns in the history of carnivorous mammals. *Annual Review*  
511 *of Earth and Planetary Sciences*, **27**, 463-493 (1999).

512

513

514 **Data accessibility.** All data files are available via the following link:

515 <https://beardatashare.bham.ac.uk/getlink/fiR7wvK357hbPrQ9FVg6eR1Q/> Upon acceptance the  
516 files will be moved to a permanent repository (e.g. Dryad).

517 **Authors' contributions.** S.L conceived the study and designed the analyses. S.L., D.D.C and  
518 T.L.S. conducted the analyses and designed the figures. B.F and E.-M.B. contributed to the datasets.  
519 All authors contributed to the writing of the manuscript.

520 **Competing interests.** We declare we have no competing interests.

521 **Funding.** T.L.S. was funded by ERC grant 788203 (INNOVATION). B.F. was funded by the  
522 Spanish Ministry of Science and Competitiveness (Grants CGL2015-68300P; CGL2017-92166-  
523 EXP).

524 **Acknowledgements.** The authors are very grateful to Armin Elsler (University of Bristol) for  
525 sharing R code that aids the processing and plotting of outputs from BayesTraits. Part of this work  
526 was carried out using the computational facilities of the Advanced Computing Research Centre,  
527 University of Bristol. Jordi Marcé-Nogue and Robert Brocklehurst are thanked for constructive  
528 suggestions improving the manuscript.

529



530 **Figure captions**

531 **Figure 1:** Sabre-toothed vertebrates in their phylogenetic context. Taxa are represented by skull  
532 outlines with the mandible opened at the maximum gape angle. Composite phylogenetic tree based  
533 on [34-36].

534

535 **Figure 2:** Biomechanical performance for different sabre-toothed clades through time: (a) actual  
536 (solid lines) and effective (dotted lines) gape angle; (b) average bending strength of the mandible  
537 tested in non-masticatory scenario; (c) relative bite force (bite efficiency) based on ratio between  
538 absolute bite forces and muscle forces.

539

540 **Figure 3:** Morphospace and performance space occupation of studied sabre-tooth species (crania  
541 and mandibles combined): (a) morphospace with convex hulls for different groups obtained from  
542 the Procrustes coordinates of the landmark analysis; (b) performance heatmap with actual gape  
543 angle values plotted onto morphospace; (c) performance heatmap with effective gape angle values  
544 plotted onto morphospace; (d) performance heatmap with bending strength values plotted onto  
545 morphospace; (e) performance heatmap with bite force values plotted onto morphospace.  
546 Phylogenetic relationships as in fig. 1 superimposed on heatmaps.

547

548 **Figure 4:** Rates of biomechanical evolution in sabre-toothed vertebrates: (a) rates of evolution in  
549 gorgonopsian gape angle summarised from 97 heterogeneous rate trees; (b) evolutionary rates in  
550 sabre-toothed mammal gape angle showing the consensus tree from 58 heterogeneous rate trees; (c)  
551 rates of evolution in sabre-toothed mammal bending strength summarised from 97 heterogeneous  
552 rate trees; (d) evolutionary rates in sabre-toothed mammal bite force illustrating consensus results  
553 from 94 heterogeneous rate trees. Rates of evolution in gorgonopsian bending strength and bite  
554 force were homogeneous. In each plot, phylogenetic branches and tip labels are coloured according  
555 to evolutionary rates, grading from slow to fast as denoted by the keys. The branch lengths are  
556 scaled to time and based on the average lengths from the time-scaled input trees. Results were  
557 consistent in both the 'equal' and FBD dated trees (figure S12).

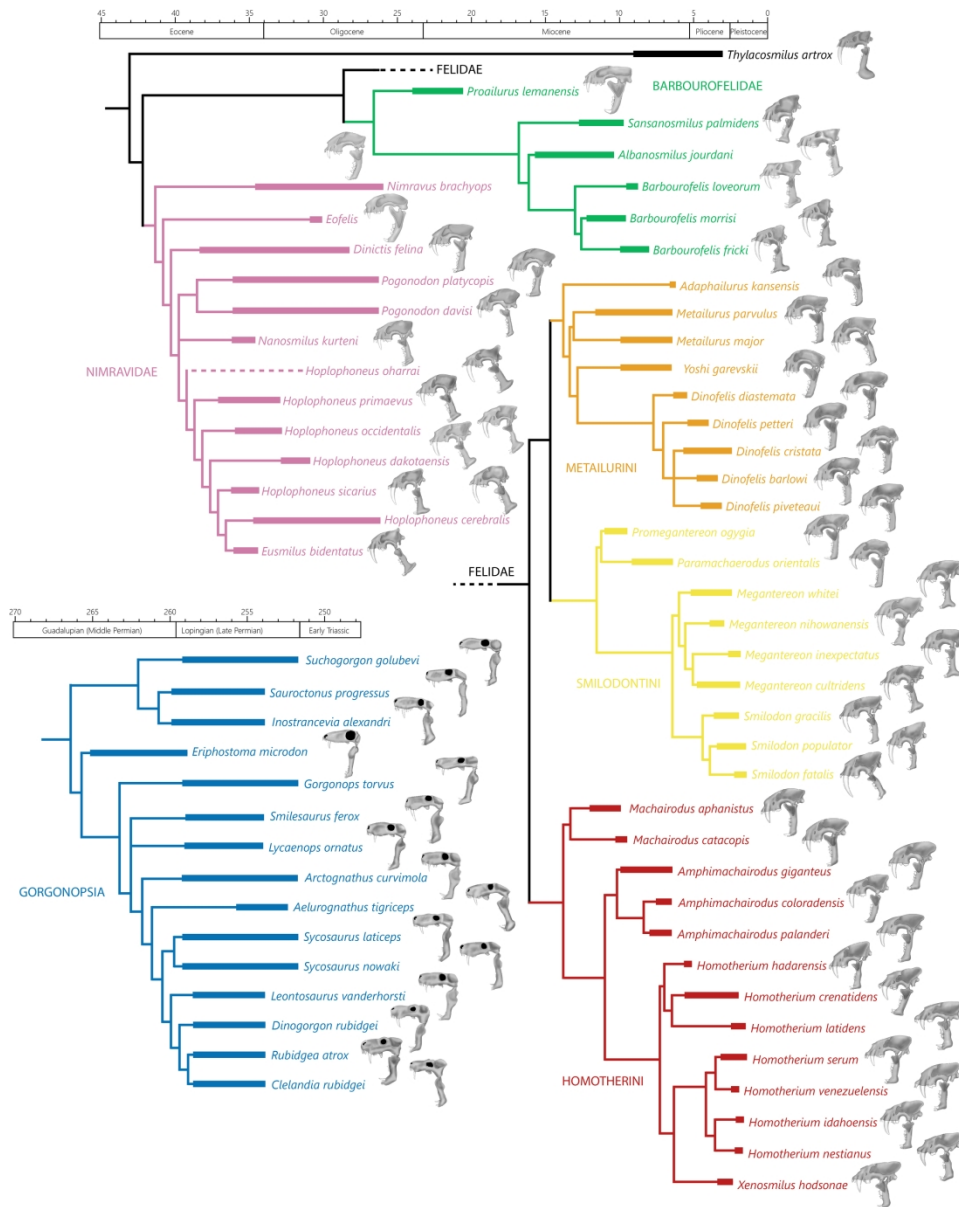


Figure 1: Sabre-toothed vertebrates in their phylogenetic context. Taxa are represented by skull outlines with the mandible opened at the maximum gape angle. Composite phylogenetic tree based on [34-36].

209x262mm (300 x 300 DPI)

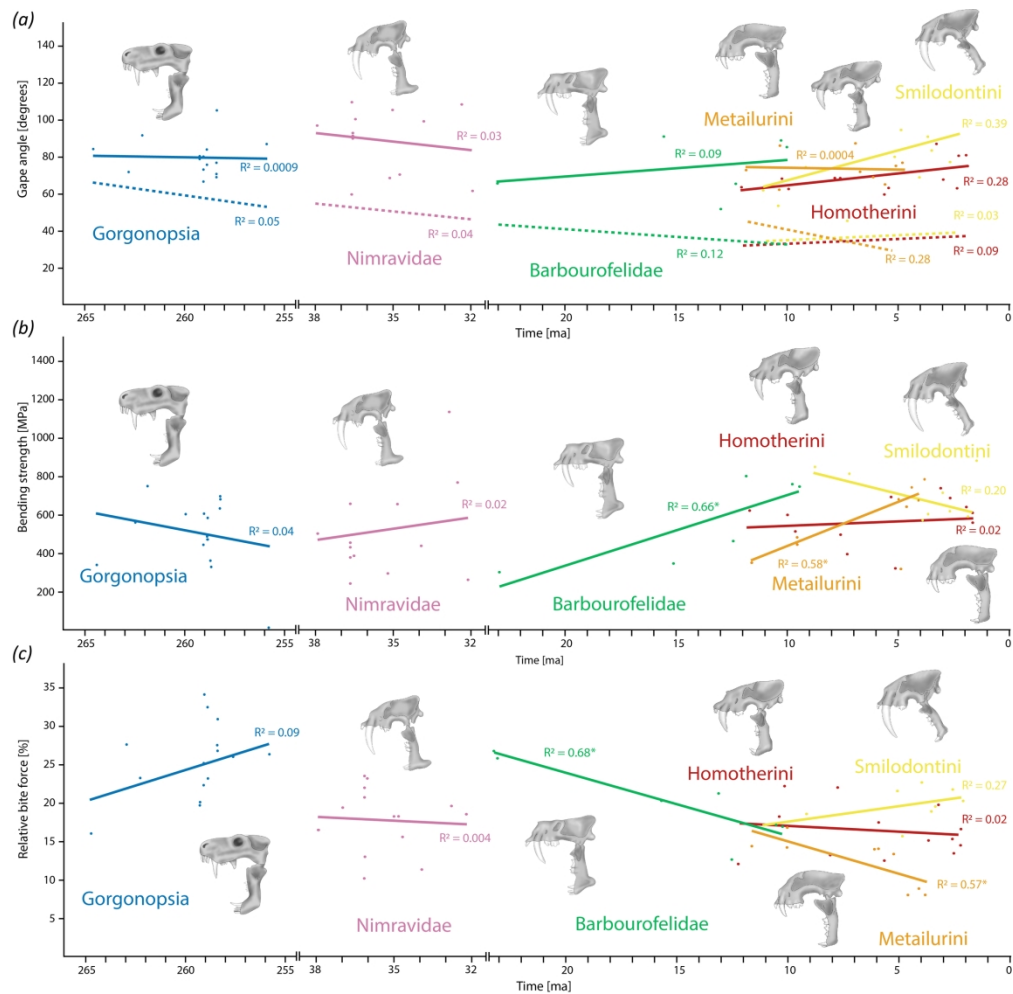


Figure 2: Biomechanical performance for different sabre-toothed clades through time: (a) actual (solid lines) and effective (dotted lines) gape angle; (b) average bending strength of the mandible tested in non-masticatory scenario; (c) relative bite force (bite efficiency) based on ratio between absolute bite forces and muscle forces.

212x208mm (300 x 300 DPI)

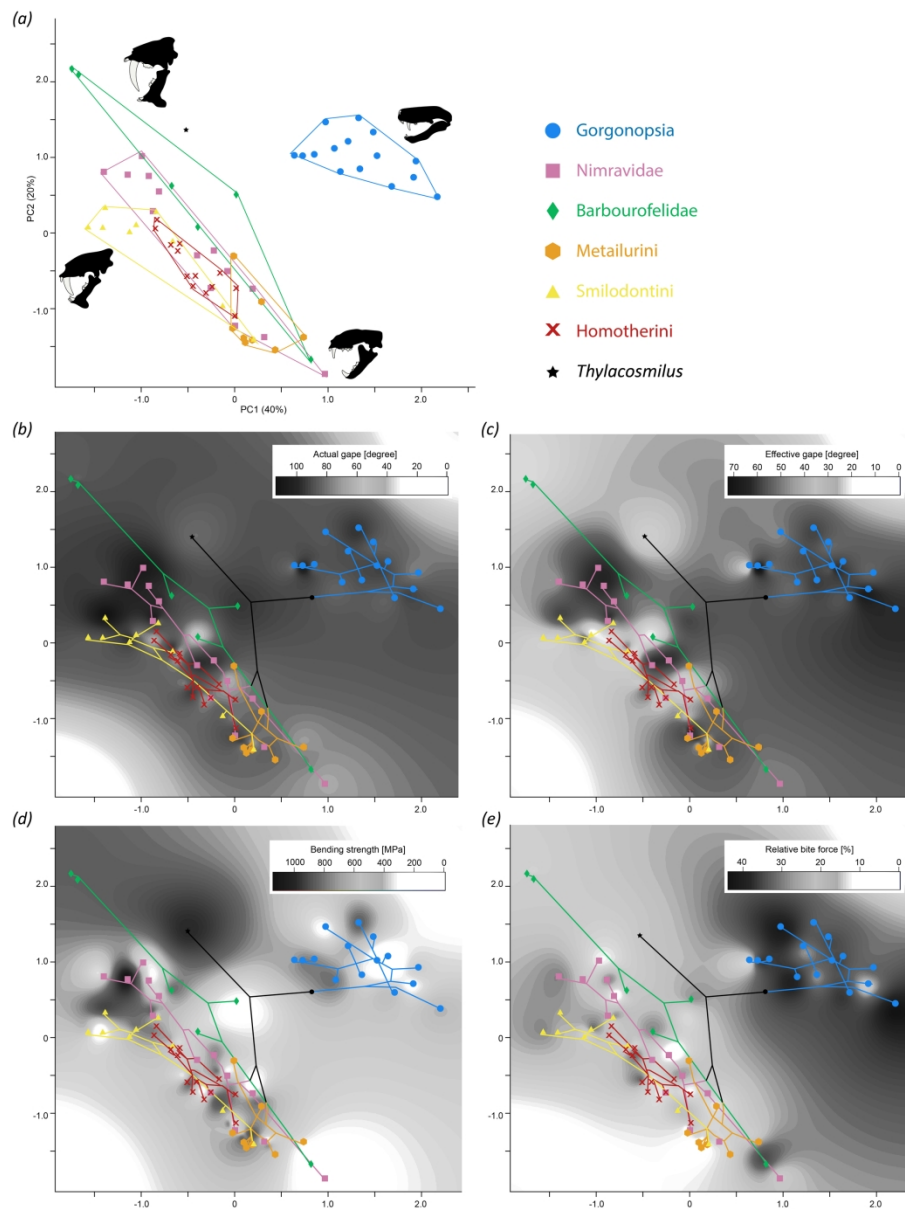


Figure 3: Morphospace and performance space occupation of studied sabre-tooth species (crania and mandibles combined): (a) morphospace with convex hulls for different groups obtained from the Procrustes coordinates of the landmark analysis; (b) performance heatmap with actual gape angle values plotted onto morphospace; (c) performance heatmap with effective gape angle values plotted onto morphospace; (d) performance heatmap with bending strength values plotted onto morphospace; (e) performance heatmap with bite force values plotted onto morphospace. Phylogenetic relationships as in fig. 1 superimposed on heatmaps.

211x279mm (300 x 300 DPI)

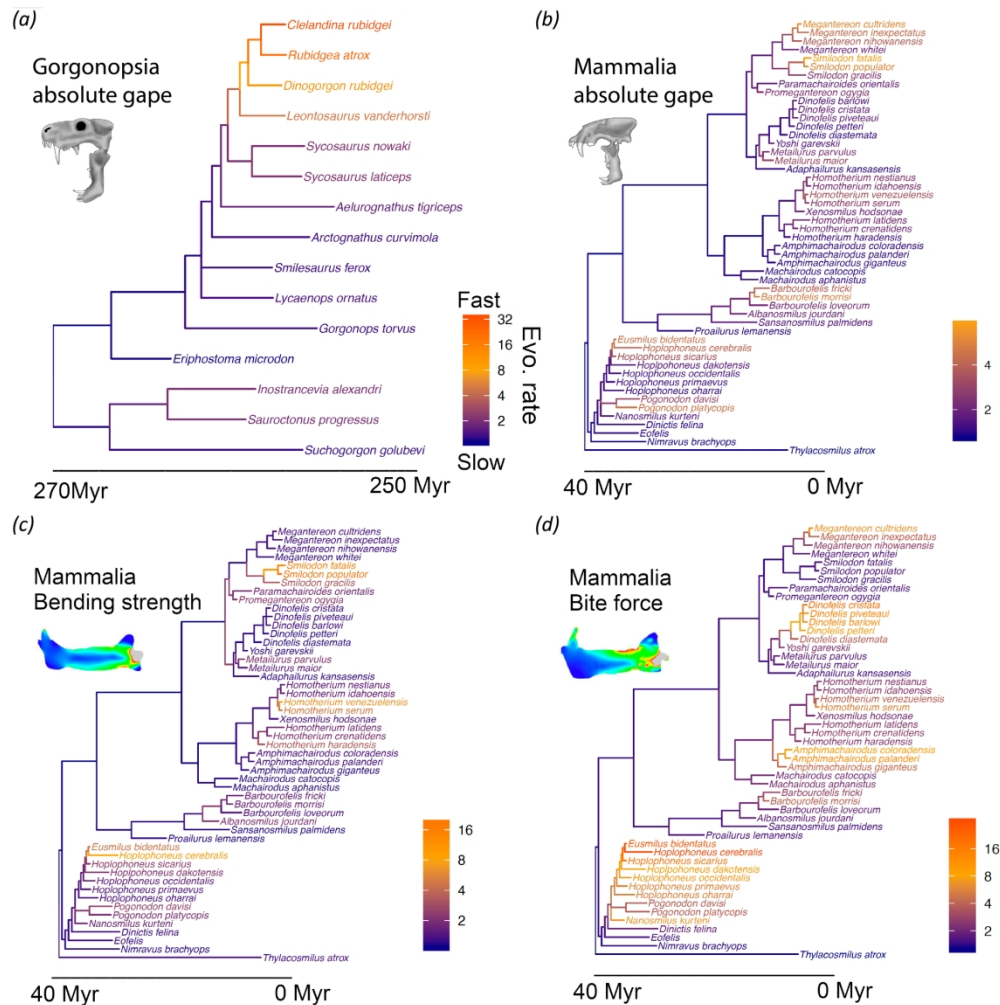


Figure 4: Rates of biomechanical evolution in sabre-toothed vertebrates: (a) rates of evolution in gorgonopsian gape angle summarised from 97 heterogeneous rate trees; (b) evolutionary rates in sabre-toothed mammal gape angle showing the consensus tree from 58 heterogeneous rate trees; (c) rates of evolution in sabre-toothed mammal bending strength summarised from 97 heterogeneous rate trees; (d) evolutionary rates in sabre-toothed mammal bite force illustrating consensus results from 94 heterogeneous rate trees. Rates of evolution in gorgonopsian bending strength and bite force were homogeneous. In each plot, phylogenetic branches and tip labels are coloured according to evolutionary rates, grading from slow to fast as denoted by the keys. The branch lengths are scaled to time and based on the average lengths from the time-scaled input trees. Results were consistent in both the 'equal' and FBD dated trees (figure S12).

209x209mm (300 x 300 DPI)